Electronic Supplementary Material (ESI) for Nanoscale Advances.
This journal is © The Royal Society of Chemistry 2020

Optimization of Electron Beam-Deposited Silver Nanoparticles on Zinc Oxide for Maximally Surface Enhanced Raman Spectroscopy

Andrew L Cook, Christopher P Haycook, Richard R Mu, Andrea K Locke, and Todd D Giorgio

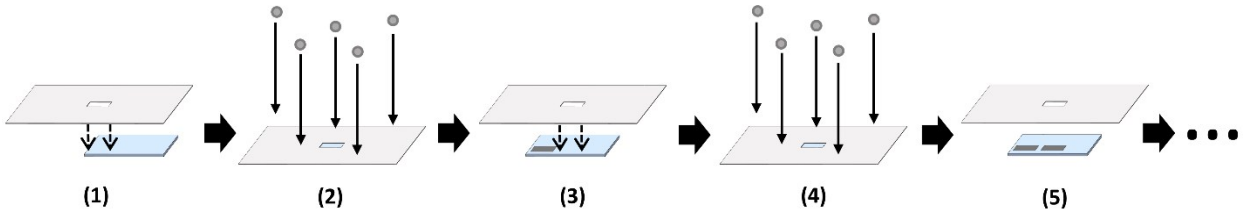

Figure S1: Illustration of the Ag deposition process. Masks cut from aluminum foil were placed on top of each substrate in step (1) such that only a small portion of the substrates was exposed. Ag was then e-beam deposited in step (2), after which the masks were moved to expose a new portion of each substrate in step (3). Ag was again deposited in step (4), and the process was repeated from step (5) onward until 9 Ag films of different thicknesses were deposited on each substrate.

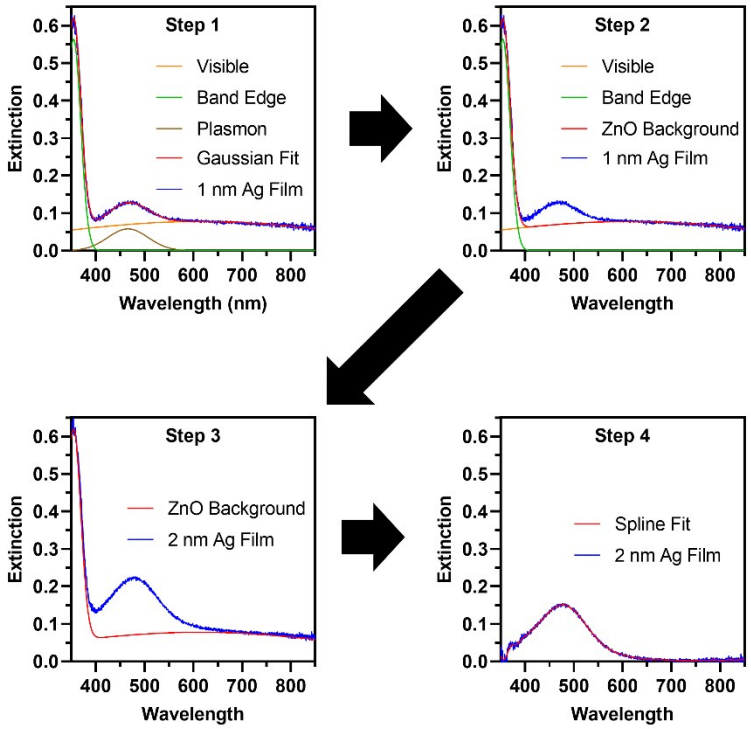

Figure S2: Process for isolating Ag nanoparticle plasmon extinction, in which (Step 1) extinction spectra for 1-nm Ag films on each substrate were approximated with a tri-gaussian fit, (Step 2) the gaussian peaks associated with ZnO background were determined and summed, then (Step 3) subtracted from each film thickness on each substrate. The resultant plasmon peak was (Step 4) approximated with a spline fit to determine peak information.

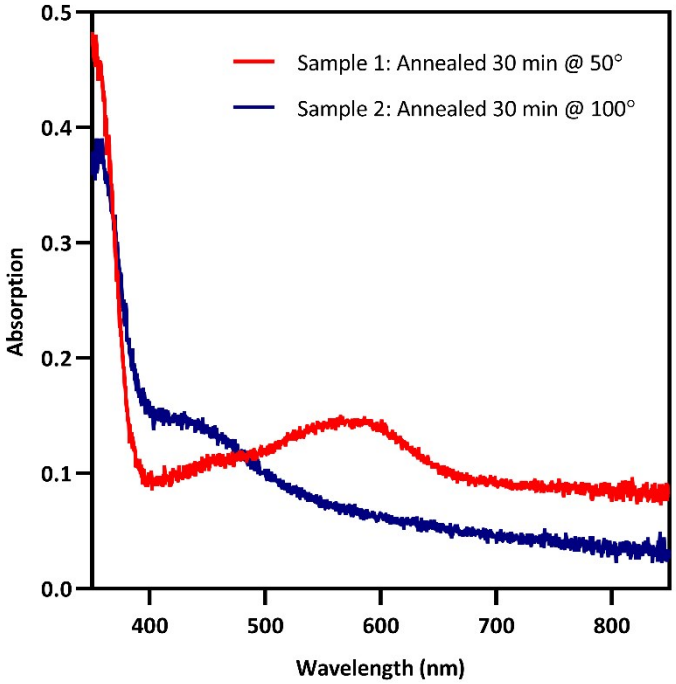

Figure S3: UV-Vis of two Ag-decorated ZnO samples, illustrating the variability in ZnO absorptive background induced by the fabrication and anneal process

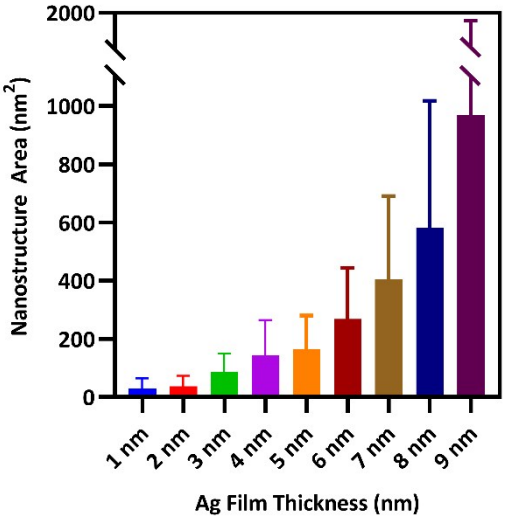

Figure S4: Average area of nanostructures for each Ag film thickness, demonstrating increasing nanostructure size with increasing film thickness.

Table S1: Benzene and non-benzene vibrational modes associated with crystal violet Raman peaks. γ = torsion, δ = bending, ν = stretching, σ = scissoring, ρ = rocking; *s* = symmetric, *as* = asymmetric

Raman Band (cm^{-1})	**Non-Benzene Vibrational Modes**	**Benzene Modes**	**Reference**
208	γ(C-H)/whole molecule breathing		[1]
225	ν_s(C-C_{center}-C)		[2]
345	γ(C-N-C)/δ(C-C_{center}-C)		[1–5]
420	δ(C-C_{center}-C)/δ(C-N-C)	16a	[1–4, 6]
441	δ(C-C-C)$_{ring,\perp}$/δ(C-N-C)/δ_{as}(C-C_{center}-C)$_{\perp}$	16a	[1, 4–6]
525	δ(C-N-C)	16b,6b	[1, 3, 4]
571	δ(C-C-C)$_{\perp}$/δ(C-N-C)/δ(C-C_{center}-C)	6a	[1, 3, 4]
605	δ(C-C-C)/δ(C-N-C)/ν_s(C-C_{center}-C)	6a	[1, 4]
623		6b	[1]
730	ν_s(C-N-C)	4,17b	[1, 2, 4]
761	ν_s(C-C_{center}-C)/ν(C-N-C)	6a,17a	[1, 2, 4]
810		10a	[1–4, 6, 7]
825		10b,17b	[1, 3, 4]
915	δ(C-C_{center}-C)	12,17a	[1, 3, 4, 6]
980		17a,18a	[1, 4]
990	δ(C-C-C)	1	[1, 4]
1130	δ(C-C_{center}-C)/ν(C-N)	15	[1, 2]
1175	ν_{as}(C-C_{center}-C)	9a,9b	[1–7]
1300	ν(C-C-C)/δ(C-C-C)$_{ring}$/δ(C-H)		[1, 2, 7]
1345	δ(C-N)/δ(C-C-C)$_{ring}$/ν_{as}(C-C_{center}-C)/δ(C-H)		[1]
1374	ν(C-N)/ν_{as}(C-C_{center}-C)/δ(C-H)		[1–7]
1445	δ_{as}(C-H_3)	19b	[1–4]
1490	δ_{as}(C-H_3)	19a	[1, 3, 4]
1529	ν(C_{ring}-N)/δ_s(C-H_3)	8b	[1, 2, 5–7]
1592		8a	[1, 2, 4–7]
1621		8a	[1, 2, 4–7]

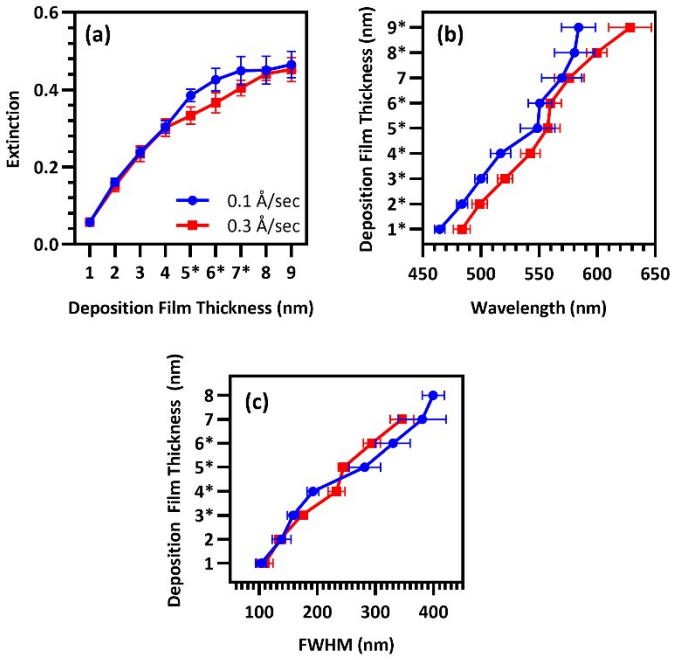

Figure S5: Means of (a)peak intensity (n = 40), (b)plasmon peak wavelength (n = 40), and (c)plasmon peak FWHM for each film thickness of Group A (blue) and Group B (red). Statistical testing performed with two-way ANOVA, *p = 0.05.

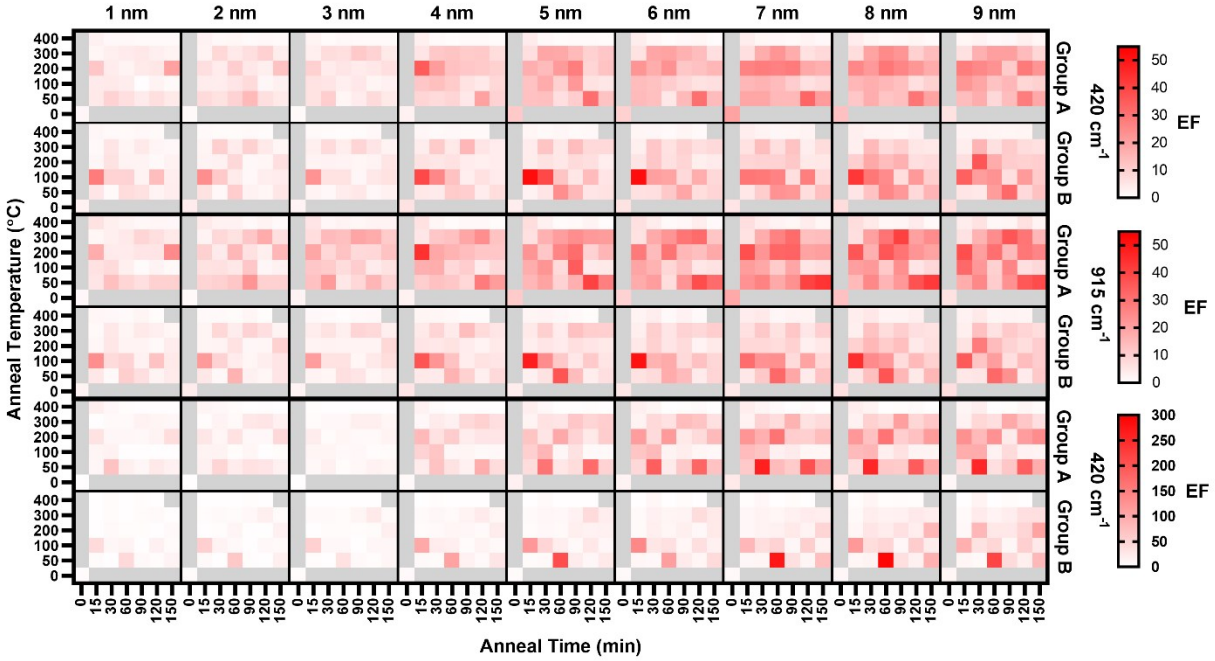

Figure S6: Enhancement Factors for three analyzed peaks of the CV SERS spectra of each film thickness on each annealed substrate and the unannealed control for each rate group.

References

1. Cañamares MV, Chenal C, Birke RL, Lombardi JR (2008) DFT, SERS, and Single-Molecule SERS of Crystal Violet. J Phys Chem C 112:20295–20300. https://doi.org/10.1021/jp807807j
2. Liang EJ, Ye XL, Kiefer W (1997) Surface-Enhanced Raman Spectroscopy of Crystal Violet in the Presence of Halide and Halate Ions with Near-Infrared Wavelength Excitation. J Phys Chem A 101:7330–7335. https://doi.org/10.1021/jp971960j
3. Watanabe T, Pettinger B (1982) Surface-enhanced Raman scattering from crystal violet adsorbed on a silver electrode. Chemical Physics Letters 89:501–507. https://doi.org/10.1016/0009-2614(82)83054-6
4. Angeloni L, Smulevich G, Marzocchi MP (1979) Resonance Raman spectrum of crystal violet. J Raman Spectrosc 8:305–310. https://doi.org/10.1002/jrs.1250080603
5. Harraz FA, Ismail AA, Bouzid H, et al (2015) Surface-enhanced Raman scattering (SERS)-active substrates from silver plated-porous silicon for detection of crystal violet. Applied Surface Science 331:241–247. https://doi.org/10.1016/j.apsusc.2015.01.042
6. Meng W, Hu F, Zhang L-Y, et al (2013) SERS and DFT study of crystal violet. Journal of Molecular Structure 1035:326–331. https://doi.org/10.1016/j.molstruc.2012.10.066
7. Wang J, Gao X, Sun H, et al (2016) Monodispersed graphene quantum dots encapsulated Ag nanoparticles for surface-enhanced Raman scattering. Materials Letters 162:142–145. https://doi.org/10.1016/j.matlet.2015.09.127